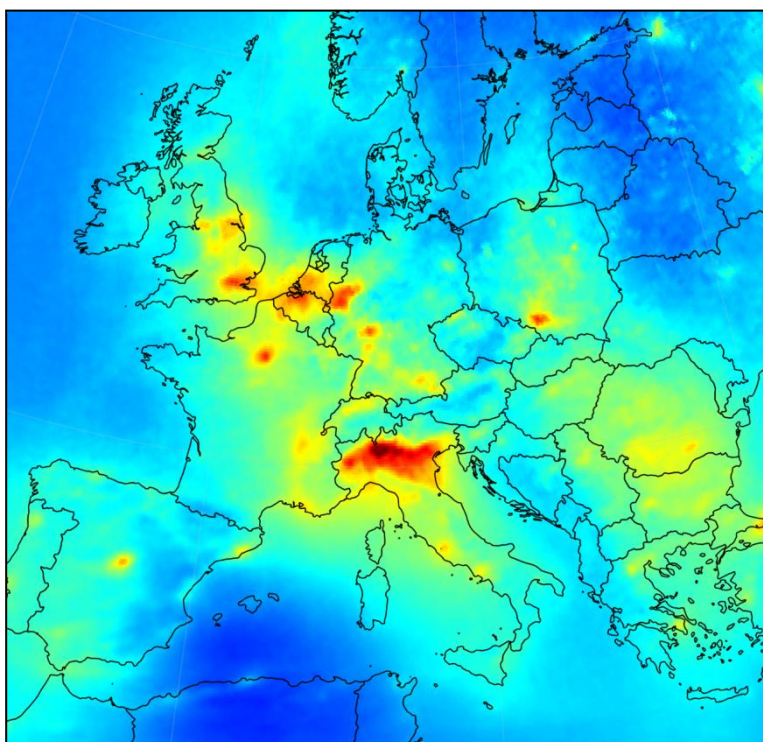


The potential of GMES satellite data for mapping nitrogen dioxide at the European scale



ETC/ACM Technical Paper 2012/9
December 2012

Philipp Schneider, Leonor Tarrasón, and Cristina Guerreiro



The European Topic Centre on Air Pollution and Climate Change Mitigation (ETC/ACM)
is a consortium of European institutes under contract of the European Environment Agency
RIVM UBA-V ÖKO AEAT EMISIA CHMI NILU VITO INERIS 4Sfera PBL CSIC

Front page picture:

Average NO₂ concentration for 2009 mapped by geostatistical techniques using Airbase station observation and data from the Ozone Mapping Instrument (OMI) as an auxiliary dataset.

Author affiliation:

Philipp Schneider, Leonor Tarrasón, and Cristina Guerreiro: Norwegian Institute for Air Research (NILU)

DISCLAIMER

This ETC/ACM Technical Paper has not been subjected to European Environment Agency (EEA) member country review. It does not represent the formal views of the EEA.

© ETC/ACM, 2012.

ETC/ACM Technical Paper 2012/9

European Topic Centre on Air Pollution and Climate Change Mitigation

PO Box 1

3720 BA Bilthoven

The Netherlands

Phone +31 30 2748562

Fax +31 30 2744433

Email etcacm@rivm.nl

Website <http://acm.eionet.europa.eu/>

The potential of GMES satellite data for mapping nitrogen dioxide at the European scale

Philipp Schneider¹, Leonor Tarrasón¹, and Christina Guerreiro¹

¹*NILU - Norwegian Institute for Air Research, Kjeller, Norway*

Abstract

The potential of future satellite retrievals of NO₂ as collected within the Global Monitoring for Environment and Security (GMES) initiative for purposes of European-scale mapping of air quality is assessed. After comparing several existing NO₂ datasets from different instruments with respect to their suitability for simulating Sentinel-5 precursor data in the mapping procedure, the daily 0.1 degree resolution OMNO2e dataset produced by the National Aeronautics and Space Administration (NASA) was selected for further processing. Annual mean station data for 2009 was combined with the satellite NO₂ data as an auxiliary variable using geostatistical techniques. More specifically, residual kriging was used. The results were compared to an equivalent approach using high-resolution model output as an auxiliary dataset. The results indicate that satellite data giving NO₂ tropospheric columns at a spatial resolution of approximately 10 km × 10 km provide significant improvements in mapping accuracy as compared to geostatistical interpolation of solely station data. While not quite reaching the accuracy level of using high-resolution model output as an auxiliary dataset, satellite-based tropospheric column data of NO₂ is shown to be a suitable proxy for obtaining spatial information for mapping purposes, when such highly-detailed model data is not available as is often the case due to the high demands on computational resources.

Contents

1	Introduction	7
2	Data	8
2.1	Airbase Data	9
2.2	Satellite Data	10
2.3	Model data	11
3	Methodology	12
3.1	Satellite Retrieval Methodology	12
3.2	Geostatistical framework	13
3.3	Cross-Validation	15
4	Results and Discussion	16
4.1	Choice of satellite product	16
4.2	Mapping using only station data	23
4.3	Mapping using station and sat. data	24
4.4	Comparison of mapping techniques	26
5	Conclusions	31
5.1	Summary	31
5.2	Recommendations	32

List of Figures

1	Map showing the 2009 average surface NO ₂ concentration measured at all Airbase background stations.	9
2	Example of an empirical semivariogram $\hat{\gamma}(h)$ and its model	15
3	Annual mean tropospheric column of NO ₂ for the year 2009 derived from the OMNO2e daily 0.25° × 0.25° product	16
4	Annual mean tropospheric column of NO ₂ for the year 2009 derived from the SCIAMACHY/TEMIS monthly 0.25° × 0.25° product	17
5	Difference image of the mean annual NO ₂ column retrieved from SCIAMACHY and OMI	20
6	The 0.1° × 0.1° resolution OMINO2e product over Europe	21
7	Comparison of the 0.25 degree resolution OMNO2e product (top) with the 0.1 degree resolution OMNO2e product (bottom), shown for the Po valley region in Northern Italy	22
8	Ordinary kriging of Airbase station data only. No auxiliary data was used in this approach.	23
9	Scatterplot of Airbase-derived annual mean 2009 station NO ₂ concentration against the 2009 annual mean tropospheric NO ₂ columns derived from the OMNO2e high-resolution product.	25
10	Empirical and modeled semivariogram of the residuals	26
11	Map of the 2009 annual average NO ₂ concentration computed as the result from kriging station data from Airbase using the OMNO2e satellite product as an auxiliary dataset	27
12	As Figure 11 but showing more detail in the spatial patterns, for the regions of a) Belgium/Netherlands, b) Northern Italy, c) London, and d) Central Spain.	28
13	Annual mean NO ₂ concentration at ground level for the year 2009 as as calculated from Airbase station data and EC4MACS project results using residual kriging.	29

List of Tables

1	Overview of the primary past and current sensors used for NO ₂ monitoring from space.	11
2	Root mean squared error statistics for the different mapping approaches	30

Acronyms

AirBase	European Air quality dataBase
AMF	Air-Mass Factor
CTM	Chemical transport model
DOAS	Differential Optical Absorption Spectroscopy
EC4MACS	European Consotrium for Modelling Air pollution and CLi- mate Strategies
EEA	European Environmental Agency
EMEP	European Monitoring and Evaluation Programme
Envisat	Environmental Satellite
ETC/ACM	European Topic Centre for Air Pollution and Climate Change Mitigation
GMES	Global Monitoring for Environment and Security
GOME	Global Ozone Monitoring Experiment
GOME-2	Global Ozone Monitoring Experiment-2
INERIS	Institute National de l'EnviRonnement industriel et des rISques
NASA	National Aeronautics and Space Administration
NIR	Near infrared
OMI	Ozone Monitoring Instrument
RMSE	Root Mean Squared Error
SCIAMACHY	SCanning Imaging Absorption spectroMeter for Atmo- spheric CartographY
TEMIS	Tropospheric Emission Monitoring Internet Service
TROPOMI	TROPOspheric Monitoring Instrument
UV	Ultraviolet
VIS	Visible

1 Introduction

Mapping air quality in Europe has been a very important focus of the work carried out by the European Topic Centre for Air Pollution and Climate Change Mitigation (ETC/ACM) in previous years (Horálek et al., 2007, 2008, 2010; De Smet et al., 2009, 2010; Denby et al., 2010, 2011a,b). A variety of mapping approaches and a multitude of input datasets have been utilized within the ETC/ACM mapping activities and over the years a reliable and mature methodology has been developed. The maps resulting from applying this methodology are provided annually by the European Environment Agency to the end-user on an operational basis (for example at <http://www.eea.europa.eu/data-and-maps/figures/pm10-annual-average-2009>).

While Europe-wide station data provides the core information for the mapping procedure, auxiliary data is generally needed to provide additional information about spatial patterns of the parameter in question. The current mapping approach (Horálek et al., 2010) uses therefore also auxiliary data in the form of model output generated by the Unified EMEP atmospheric chemistry model (Simpson et al., 2003; Fagerli et al., 2004), provided at spatial resolution of $50 \text{ km} \times 50 \text{ km}$, as well as digital elevation models and data on population density.

One potential source of spatial information on air quality that has so far not been considered as an input to the ETC/ACM mapping procedure, is satellite data. Satellite data on air quality is generally considered challenging to work with as the temporal and spatial domains of the observations differ substantially from regular station observations. In addition, many satellite products are still associated with high uncertainties. However, the products are continuously improving and several revolutionary new spaceborne instruments will be launched in the next decade. These new instruments have a very high potential for providing crucial information on mapping air quality at the continental and possibly even at the urban scale.

While a strong focus of the ETC/ACM task 1.0.2.8 (“Urban air pollution assessment and links to GMES Atmospheric Service”) lies on urban-scale mapping of air quality, the use of satellite data for urban-scale applications is still highly challenging. While high-resolution urban-scale satellite mapping of particulate matter has been shown to be feasible under certain circumstances (Glantz et al., 2009), true urban-scale mapping of reactive gases from spaceborne instruments is currently not possible due to the generally coarse spatial resolution of the existing instruments. The spatial resolutions of nadir pixels for current instruments generally range from $13 \text{ km} \times 24 \text{ km}$ (OMI) over $30 \text{ km} \times 60 \text{ km}$ (SCIAMACHY) to $40 \text{ km} \times 80 \text{ km}$ (GOME-2), which is not suitable for urban-scale mapping. For this reason, this study focuses on mapping air quality and in particular NO_2 at the European scale and at a

resolution comparable to what is currently provided within the operational systems provided by the ETC/ACM (Horálek et al., 2010).

Future satellite instruments such as the TROPOMI instrument onboard of the Sentinel-5 precursor mission (van Weele et al., 2008; Veefkind et al., 2012) and the Sentinel-5 mission (Ingmann et al., 2012; Berger et al., 2012) to be launched respectively in ~2015 and ~2020 within the framework of the Global Initiative for Environment and Security (GMES) (Aschbacher and Milagro-Pérez, 2012), are designed to allow NO₂ mapping at spatial resolutions of up to 7 km × 7 km. As such they will achieve similar levels of spatial detail as are currently provided by high-resolution air quality calculations such as those provided by INERIS within the framework of the EC4MACS project. In addition, a dedicated UV/VIS instrument onboard of the geostationary Sentinel-4 platform will allow for spatially and temporally continuous mapping of NO₂ and deliver important information on daily concentration cycles. Furthermore, first airborne missions for mapping NO₂ are now offering sub-meter resolution and promise to be very valuable for true urban-scale mapping of NO₂ hotspots at some point in the future (Popp et al., 2012).

The main goal of ETC/ACM 1.0.2.8 Subtask 2 was to evaluate the use of satellite observations collected within the framework of the GMES initiative (Aschbacher and Milagro-Pérez, 2012) for their suitability in improving spatio-temporal air quality estimates at the European scale. More specifically the objectives of the work reported here were the following:

1. Identify a suitable satellite product
2. Develop a methodology to combine station observations with satellite retrievals of NO₂ to produce European-scale air quality maps
3. Validate the resulting map using station data
4. Perform a comparison of satellite-based vs. model-based mapping

The work presented here focuses solely on NO₂ as this is generally one of the most mature air quality-related products available from satellite observations and thus inhibits comparatively low uncertainties. However, future work could explore the use of satellite-retrieved O₃ and other species in European-scale mapping.

2 Data

A wide variety of data sources were used within this study. This include station data, satellite data, and output from chemical transport models. The various primary datasets are described in detail in the following sections.

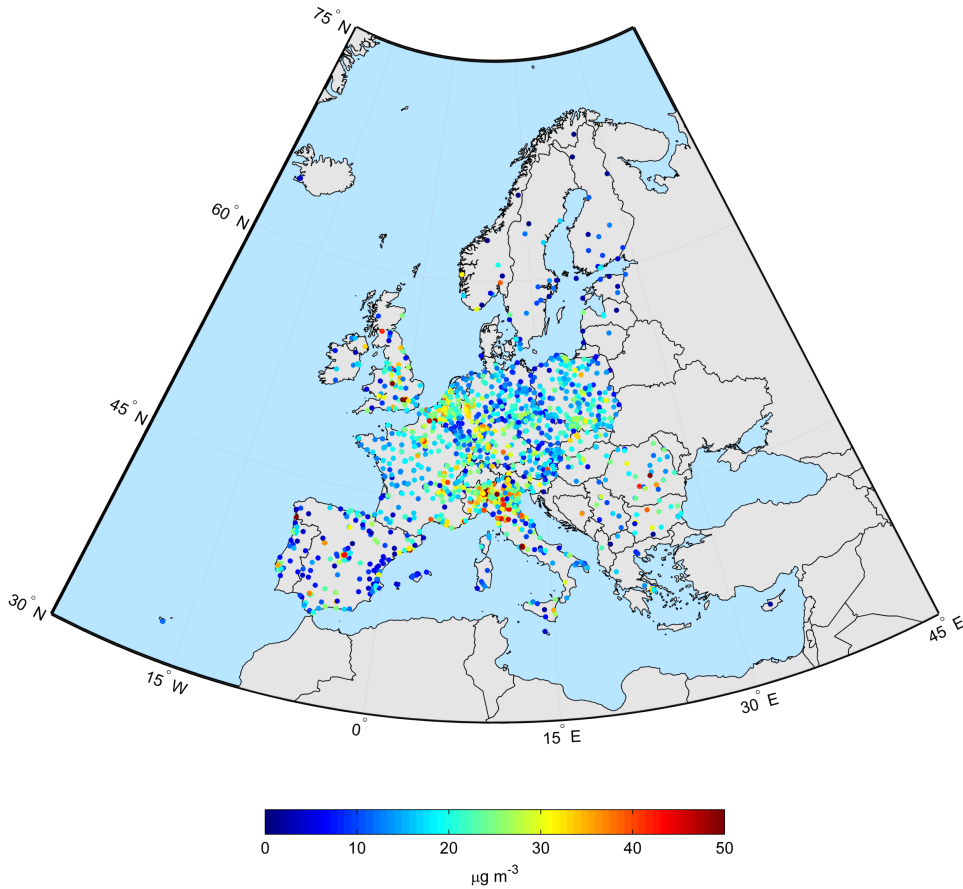


Figure 1 – Map showing the 2009 average surface NO₂ concentration measured at all Airbase background stations.

2.1 Airbase Data

Raw data from air quality stations located throughout Europe were used as a basis for spatial mapping using residual kriging. All station data was obtained from the *European Air quality dataBase*, AirBase (<http://acm.eionet.europa.eu/databases/airbase/>). AirBase is a public database system operated by the European Environmental Agency (EEA) and provides air quality monitoring data and associated information submitted by all participating countries within Europe.

Figure 1 shows a map of the locations of all stations that were used within this study. Only background stations (urban, suburban, and rural) were used. The map further indicates the annual average NO₂ concentration for 2009 as measured at the stations.

As most spatial datasets, the NO₂ data at the European station network exhibits spatial autocorrelation. Figure 2 in Section 3.2 quantifies this effect by showing the empirical semivariogram and its model of the station datasets shown in Figure 1. The spatial autocorrelation of this dataset was modeled with a nugget effect of 74.7 and a spherical model with range 13.9 degrees and a sill of 40.6.

A total of 3889 stations were considered, however only a subset of 1603 stations provided an annual mean NO₂ concentration for the year 2009, which was chosen as a reference year for this study as both a high-resolution satellite dataset as well as high-resolution model output was available for this year. No additional quality control of the data beyond what is being carried out by the member states and by EEA was undertaken.

2.2 **Satellite Data**

Operational satellite remote sensing of NO₂ has been carried out since 1995 when the Global Ozone Monitoring Experiment (GOME) (Burrows et al., 1999; Richter and Burrows, 2002) was first launched. Beginning in 2002, the observations were continued by the SCIAMACHY (SCanning Imaging Absorption spectroMeter for Atmospheric CartographY) sensor onboard of the Envisat platform (Bovensmann et al., 1999; Gottwald et al., 2006), and subsequently complemented in 2004 by the Ozone Monitoring Instrument (OMI) (Levelt et al., 2006) onboard of the Aura satellite operated by the National Aeronautics and Space Administration (NASA), as well as the Global Ozone Monitoring Experiment-2 (GOME-2) instrument (Munro et al., 2006) onboard of the first MetOp satellite launched in 2006. Table 1 gives an overview of the primary past and current spaceborne sensors used for NO₂ monitoring.

For this study data from SCIAMACHY and OMI were compared with respect to their suitability for mapping European-scale air quality.

SCIAMACHY (SCanning Imaging Absorption spectroMeter for Atmospheric CartographY) is a hyperspectral UV/VIS/NIR passive imaging grating spectrometer observing the wavelength range of 214–2386 nm (Bovensmann et al., 1999; Gottwald et al., 2006). Its overpass time is approximately 10:00 local time at the equator. The data acquired by the instrument has been used for a wide variety of operational and research applications (Gottwald et al., 2006). Monthly averaged SCIAMACHY NO₂ data were obtained from the Tropospheric Emission Monitoring Internet Service (TEMIS) website.

The Ozone Monitoring Instrument (OMI) is based on the experiences acquired from both GOME and SCIAMACHY. It combines their advantages, measuring the complete spectrum in the UV/VIS wavelength range at a comparatively

Table 1 – Overview of the primary past and current sensors used for NO₂ monitoring from space.

Sensor	GOME	SCIAMACHY	OMI	GOME-2
Platform	ERS-1	ENVISAT	Aura	MetOp
Data availability	1996 to 2003	2002 to 2012	2004 to present	2006 to present
Spatial resolution	320 km x 40 km	60 km x 30 km	13 km x 24 km	80 km x 40 km
Daily coverage	Near-Global	Partial (due to alternating nadir/limb observation)	Near-Global (significantly reduced due to instrument failure since 2007)	Near-Global
Overpass time	10:20 LST	10:00 LST	13:45 LST	09:30 LST

high spatial resolution of 13 km × 24 km, while providing daily global coverage. The OMI instrument is flying on the National Aeronautics and Space Administration’s Earth Observing System Aura platform as part of the A-train constellation of satellites. In contrast to the other instruments mentioned here, which have equator crossing times around 10:00 local time, OMI has an equator crossing time of approximately 13:30 LST in the afternoon, and therefore probes the Earth’s atmosphere under different conditions. Aura/OMI was launched in 2004 and has been continuously providing data. Beginning in June 2007, OMI has suffered from several row anomalies affecting the quality of the Level 1B and Level 2 data products. Level-3 product as were used for the purposes of this study are produced after filtering for the affected anomalies.

The new OMNO2e v3 product was obtained directly from contacts at NASA’s Goddard Space Flight Center, as the product was not officially publicly available yet. Two versions of the product were acquired: One gridded at a 0.25° × 0.25° spatial resolution was obtained for the entire lifetime of the OMI instrument from 2004 to present and one gridded at 0.1° × 0.1° spatial resolution was obtained for the year 2009 only. Figure 7 provides a comparison of the two products for a highly polluted area in Northern Italy.

2.3 Model data

Model output produced by INERIS for the EC4MACS project was used in this study. The EC4MACS project uses the CHIMERE model (Vautard et al., 2001; Bessagnet et al., 2004), which is a three-dimensional chemistry transport

model (CTM) that is widely used within the air quality scientific community for a variety of applications.

3 Methodology

3.1 Satellite Retrieval Methodology

Two satellite NO₂ products were further investigated for their use within this study. The first product tested was acquired by the SCIAMACHY instrument onboard of the Envisat platform. The product used is based on the TEMIS retrieval algorithm (Boersma et al., 2011).

In short, the TEMIS NO₂ retrieval is based on three steps: The first step of the algorithm consists of a Differential Optical Absorption Spectroscopy (DOAS) retrieval of the total slant column of NO₂ from the measured spectrum, where absorption cross sections of NO₂, ozone, H₂O as well as a synthetic ring spectrum are taken into account, and a fifth order polynomial is included in the fit to account for scattering effects. The second step consists of the separation of the stratospheric and tropospheric NO₂ contributions to the total NO₂ column, where the stratospheric NO₂ column is estimated by assimilating total slant columns in the TM4 chemistry transport model (Dentener et al., 2003; Boersma et al., 2007). The third and final step of the retrieval is the conversion of the tropospheric NO₂ slant columns into vertical columns using a calculated Air-Mass Factor (AMF). Further details on the specific retrieval methodology can be found in Boersma et al. (2004), Boersma et al. (2007), and Boersma et al. (2011), as well as on the TEMIS website (www.temis.nl).

Solely data reprocessed with version 2.0 of the retrieval algorithm was used. Improvements in version 2.0 over previous versions of the retrieval algorithm include an updated albedo database, a modified calculation of the air mass factor, a correction of the surface height calculation, a correction of the weekly cycle in NO_x emissions, as well as an increased number of NO_x tracers in the applied chemical transport model (Boersma et al., 2011). The NO₂ dataset used here only considered cloud radiance fractions of less than 50%. It was also resampled from the original SCIAMACHY spatial resolution to a 0.25 degree × 0.25 degree grid.

Although the TEMIS-based NO₂ dataset used in this study is based to some extent on data assimilation using the TM4 model (Dentener et al., 2003; Boersma et al., 2007), it is almost independent of the used emission inventory due to the retrieval set-up. The data assimilation results are mainly used to provide the stratospheric NO₂ column in the second step. This stratospheric column is virtually independent of the used emission database. For the

calculation of the AMF in the third step knowledge of the profile shape of the vertical NO₂ distribution is needed. This profile shape is also taken from the data assimilation. However, the profile shape is independent of the emissions, since the data assimilation is scaling the NO₂ column with conservation of the shape. In conclusion, the NO₂ data are considered as retrieval results independent of emission data.

The second satellite NO₂ product tested here was acquired by the Ozone Mapping Instrument onboard the Aura satellite. The OMI product used within the framework of this study is based on a retrieval algorithm developed at NASA (Chance, 2002). The original, version 1 retrieval algorithm is described in Bucsela et al. (2006). The new version 3.0 retrieval algorithm is greatly improved over the previous versions (Bucsela, 2012).

The retrieval algorithm for the OMI NO₂ product consists of a total of four major steps: A Differential Optical Absorption Spectroscopy, a calculation of the air mass factor, destriping, and a troposphere-stratosphere separation. The DOAS first divides earthshine radiances by the reference solar irradiance spectrum. The normalized spectra are then fitted to trace gas spectra observed in the laboratory using a reference Ring spectrum and a polynomial function. The DOAS fitting is applied in the spectral range of 405 nm to 465 nm. In a next step, the air mass factor is calculated using scattering weights and a monthly mean climatology of NO₂ profile shapes, which were derived from a chemical transport model. The AMF is subsequently computed using the cloud radiance fraction f as

$$AMF = (1 - f) \cdot AMF_{clear} + f \cdot AMF_{cloud} \quad (1)$$

where AMF_{clear} and AMF_{cloud} are the model-derived air mass factors for clear and cloudy conditions, respectively. Following the AMF calculation, the NO₂ slant column densities observed by OMI are then “destriped” in order to correct for an instrument artifact. Finally, as a fourth step, a troposphere-stratosphere separation is performed using an *a priori* estimate of the tropospheric contribution based on a monthly model climatology.

More information about the OMI NASA retrieval algorithm can be found in Bucsela et al. (2006), Bucsela (2012), and OMI Team (2012). The OMINO₂ product (Chance, 2002) is estimated to have a fitting error in the slant column of approximately $0.3 - 1 \times 10^{15}$ molecules cm⁻² (OMI Team, 2012).

3.2 Geostatistical framework

The European background maps are created using a geostatistical technique, namely residual kriging with auxiliary variables. Kriging is an interpolation technique that makes use of a model of spatial autocorrelation (usually in

the form of a variogram model) to infer optimal estimates of a variable at a given set of locations (Isaaks and Srivastava, 1989; Cressie, 1993; Goovaerts, 1997; Wackernagel, 2003).

The mapping procedure applied in this study is based on the previous work by Horálek et al. (2007), Horálek et al. (2010), and Denby et al. (2011a) and involves a linear regression analysis against an auxiliary variable in conjunction with kriging of the residuals. It should be noted that the cited work incorporates a procedure for separately mapping urban and rural areas and then combining the interpolated maps using a merging technique. This part of the algorithm was not implemented in the mapping procedure for this project.

The concentration $\hat{Z}(s_0)$ is mapped at a given location s_0 using the model

$$\hat{Z}(s_0) = c + a_1X_1(s_0) + a_2X_2(s_0) + \dots + a_nX_n(s_0) + \eta(s_0) \quad (2)$$

where c , a_1 , $a_2 \dots a_n$ are parameters of the multiple linear regression and $X_1(s_0) \dots X_n(s_0)$ are the values of the auxiliary variables used at location s_0 . Finally, $\eta(s_0)$ represents the results of the ordinary kriging of the residuals at location s_0 . While equation 2 provides a general methodology for incorporating multiple auxiliary variables, only single auxiliary variables were tested here in order to evaluate the impact of each auxiliary variable individually (with one exception mentioned later on). The first step in the process was therefore to establish a linear relationship between the annual average NO₂ concentration at each station and the respective auxiliary variable at each station. This task was performed throughout all background stations in Europe available within AirBase (with exception of those stations used for validation) in order to obtain a representative relationship.

Kriging makes use of a model describing the spatial autocorrelation. Most often, the semivariogram $\gamma(h)$ at a certain lag distance h is used to describe this. Different types of models are then fitted to the empirical semivariogram, with a spherical and Gaussian models probably being the most common. Figure 2 shows an example of the empirical semivariogram and the fitted spherical model used for residual kriging of NO₂ over Europe.

For kriging of residuals, a model was fitted to the empirical semivariogram of the residuals with a combination of a nugget effect model and a spherical or Gaussian model of range a_0 degrees and sill $c_0 \mu\text{g m}^{-3}$ such that the semivariance $\hat{\gamma}$ at lag h is given as either

$$\hat{\gamma}(h) = \begin{cases} c_0 \cdot \left[\frac{3}{2} \frac{h}{a_0} - \frac{1}{2} \left(\frac{h}{a_0} \right)^3 \right] & \text{for } h \leq a_0 \\ c_0 & \text{for } h > a_0 \end{cases} \quad (3)$$

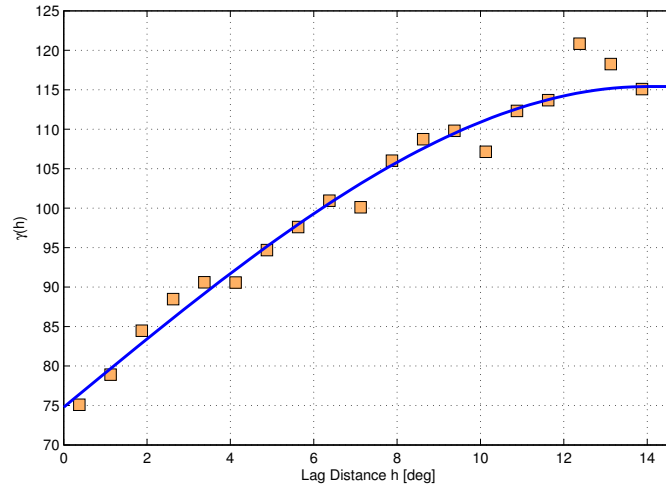


Figure 2 – Example of an empirical semivariogram $\hat{\gamma}(h)$ and its model, describing the autocorrelation of a European NO₂ station dataset. The model in this case is a combination of a nugget effect of 74.7 and a spherical model with sill 40.6 and a range of 14 degrees.

for the spherical model or

$$\hat{\gamma}(h) = c_o \left[1 - \exp\left(-\frac{h^2}{a_0^2}\right) \right] \quad (4)$$

for the Gaussian model. Many other semivariogram models exist, however these two are generally the most common and were the only ones used for the purposes of this study.

The fitted semivariogram model is then used in the kriging process to determine appropriate weighting factors for each data point. More detailed information about the kriging process can be found in the literature, e.g. in Isaaks and Srivastava (1989), Cressie (1993), or Goovaerts (1997). The kriged residuals are then added to the results from the multiple linear regression as indicated in Equation 2 and through this process the final results are obtained.

3.3 Cross-Validation

Cross-validation was used to evaluate the quality of the results. Based on this validation technique, the original Airbase dataset was randomly split up in two parts. The first part, encompassing 90% of the stations, was used within the kriging procedure. The second part, consisting of approximately 10% of the Airbase stations was used solely for validation purposes. This

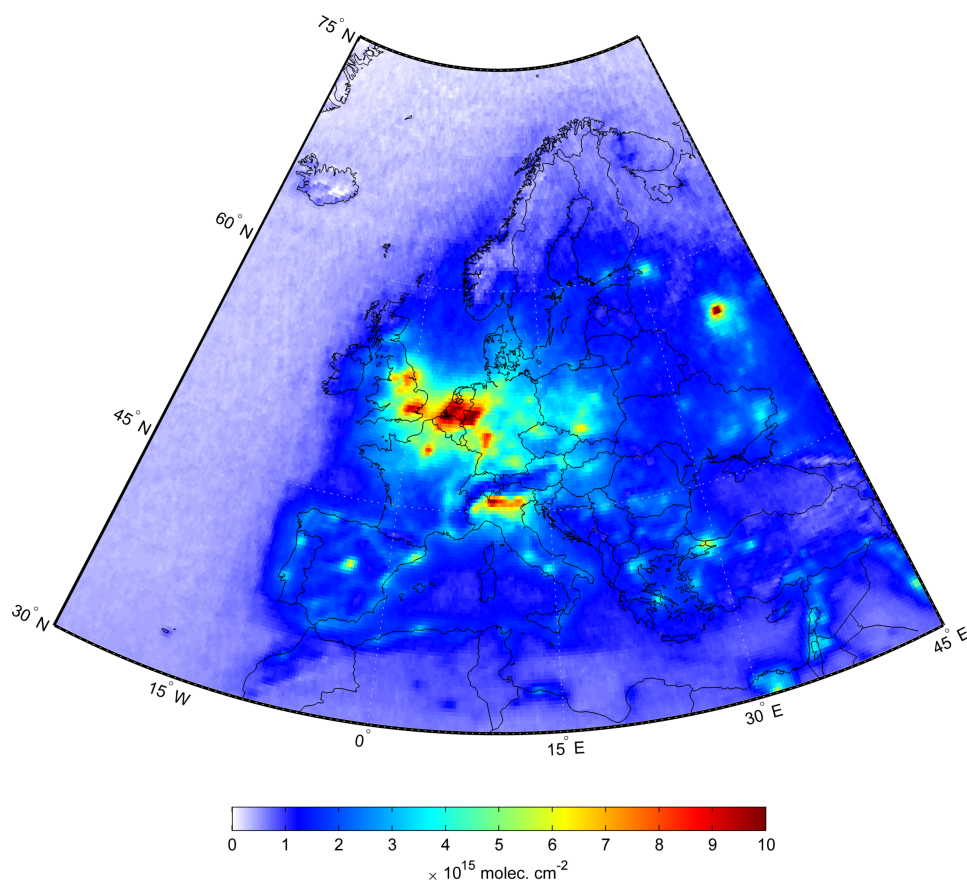


Figure 3 – Annual mean tropospheric column of NO_2 for the year 2009 derived from the OMNO2e daily $0.25^\circ \times 0.25^\circ$ product. Note that the overpass time of the Aura platform on which OMI is flying, is at approximately 13:30 local time.

procedure ensures that the stations used for validation had absolutely no impact on the quality of the result as they were not used as part of the algorithm. This resulted in a total number of 198 randomly selected stations that were separated from the main Airbase dataset and only used for validation purposes.

4 Results and Discussion

4.1 Choice of most suitable satellite product

Two satellite-based NO_2 products were chosen for further investigation: The SCIAMACHY product based on the algorithm by TEMIS (Boersma et al., 2011), and the OMNO2e product (Bucsela et al., 2006; Bucsela, 2012). Figures

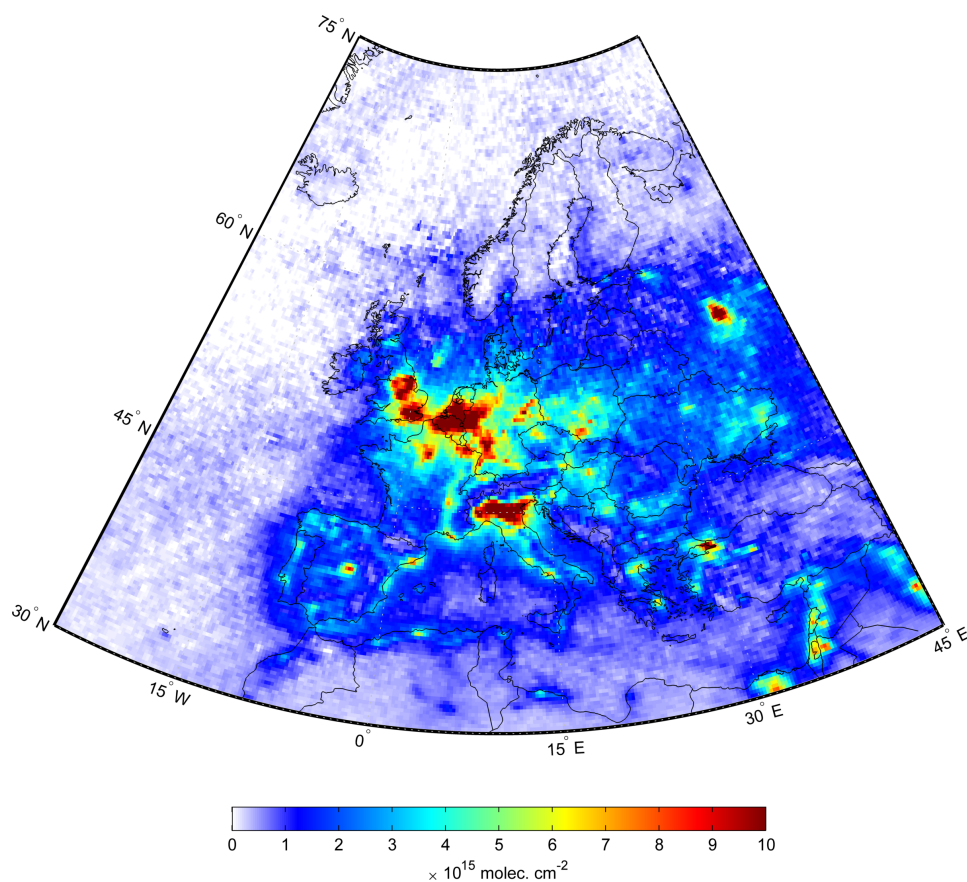


Figure 4 – Annual mean tropospheric column of NO₂ for the year 2009 derived from the SCIAMACHY/TEMIS monthly $0.25^\circ \times 0.25^\circ$ product. Note that the overpass time of the Envisat platform on which SCIAMACHY is flying, is at approximately 10:00 local time.

3 and 4 show the 2009 annual mean tropospheric NO₂ columns derived from the OMI and SCIAMACHY products using different retrieval algorithms. Note that the color scale on both figures is identical, so both qualitative and quantitative comparisons can be carried out. Overall, the spatial patterns shown by the two products agree quite well. All the major regions of generally high NO₂ concentrations, such as the region of Belgium and the Netherlands, southern and Eastern England, as well as the Po valley region in Northern Italy, are captured adequately by both products. Furthermore, individual NO₂ hotspots over more isolated cities such as Moscow, Madrid, and Istanbul are easily identifiable from both data products. The map produced from OMI data appears to be slightly smoother whereas the SCIAMACHY-based maps shows a bit more “noise”. This is due to the fact that the OMI-based annual mean map was computed by averaging over daily images, whereas

the SCIAMACHY-based annual mean was calculated from monthly average datasets, which in turn were derived from the original swath data by TEMIS.

In terms of actual NO₂ concentrations, it is obvious from the two Figures that SCIAMACHY overall measures significantly higher columns in the polluted areas than OMI. Figure 4 clearly shows this effect as significantly larger areas exceeding 10×10^{15} molecules cm⁻² as compared to 3. This effect is particularly obvious in the Po valley region in Northern Italy, for which the OMI annual mean only shows very few grid cells exceeding 10×10^{15} molecules cm⁻², whereas most of the region of Northern Italy exceeds this value in the SCIAMACHY-based map.

The reason for this behavior can be found in the combination of the strong diurnal cycle of NO₂ in heavily polluted areas and the different overpass times of the two instruments. While the Envisat satellite, on which the SCIAMACHY instrument is mounted, has a local overpass time at the equator of around 10:00 LST, and thus samples the tail end of the morning rush hour, the OMI instrument on the Aura platform has a local overpass time at the equator of approximately 13:45 LST and as such samples the atmosphere in the middle between the morning and evening rush hours. As such, its observations of tropospheric NO₂ columns are expected to be lower than those obtained from SCIAMACHY.

In order to explore the quantitative difference between the two products in more detail and with a particular focus on spatial patterns, a difference image between the products from the two instruments was produced. The difference in NO₂ column ΔC given in $\times 10^{15}$ molecules cm⁻² was calculated as

$$\Delta C = C_{SCIAMACHY} - C_{OMI} \quad (5)$$

where $C_{SCIAMACHY}$ and C_{OMI} are the annual mean NO₂ columns for SCIAMACHY and OMI, respectively. As such, positive values in the difference image indicate that the SCIAMACHY retrieval is higher than the OMI retrieval, and negative values indicate the opposite. This methodology assumes that the tropospheric NO₂ columns derived by both retrieval algorithms extend over approximately the same height and are thus comparable.

Figure 5 shows the resulting difference map. As expected, the highest absolute differences can be found over the most highly polluted areas. In Northern Italy, which exhibits the largest area of substantial differences, the values easily reach and exceed 5×10^{15} molecules cm⁻². Several regions in Germany, Belgium, the Netherlands, and the United Kingdom also reach such high values, albeit only in areas of considerably smaller spatial extent. SCIAMACHY generally shows higher tropospheric columns by approximately 1×10^{15} molecules cm⁻² on average over large areas of Eastern Europe, particularly in the Ukraine.

In areas of generally low tropospheric NO₂ concentrations such as over the oceans, Scandinavia, and Africa, OMI exhibits slightly higher values by approximately 0.5×10^{15} molecules cm⁻². However, this magnitude is easily within the error range specified for the products and thus probably is not of too much significance.

Note that, while such an inter-comparison between two satellite products is not a substitute for validation with in situ data as it can not provide an absolute error estimate, it can provide valuable information on spatial patterns in differences.

Despite differences in absolute values, it is critical to point out that the spatial patterns indicated by both instruments are very consistent. This is important because when using such satellite-based maps for supporting kriging of station data as an auxiliary datasets, it is primarily the spatial patterns that affect the results, whereas the absolute values are based on the station data.

While for the previous Figures and analysis the 0.25 degree resolution OMI product was used to provide as much consistency as possible with the SCIAMACHY product, a high-resolution 0.1 degree OMNO2e product exists for the OMI instrument. Given the similarity in spatial scale between the 0.1 degree OMNO2e product and the 10 km spatial resolution at which air quality is being mapped operationally in Europe by the ETC/ACM, this product is a natural choice for this study. Figure 7 shows a direct comparison of the two OMI products. The high resolution product clearly can resolve more detail and provides higher values in some hotspots which do not appear in the 0.25 degree resolution product due to spatial averaging.

Based on these results and further based on the fact that a 0.1 degree product was available from OMI while only 0.25 degree resolution was available from SCIAMACHY, it was decided to use the OMNO2e product for the remainder of this study. The relatively high resolution of the OMNO2e product allows for mapping at the 10 km grid cell level for all of Europe. It should further be noted that, in contrast to for example SCIAMACHY data, OMI observations are available at present and further will be continued at a higher spatial resolution in 2014 with the launch of the TROPOMI instrument onboard the Sentinel-5 precursor platform.

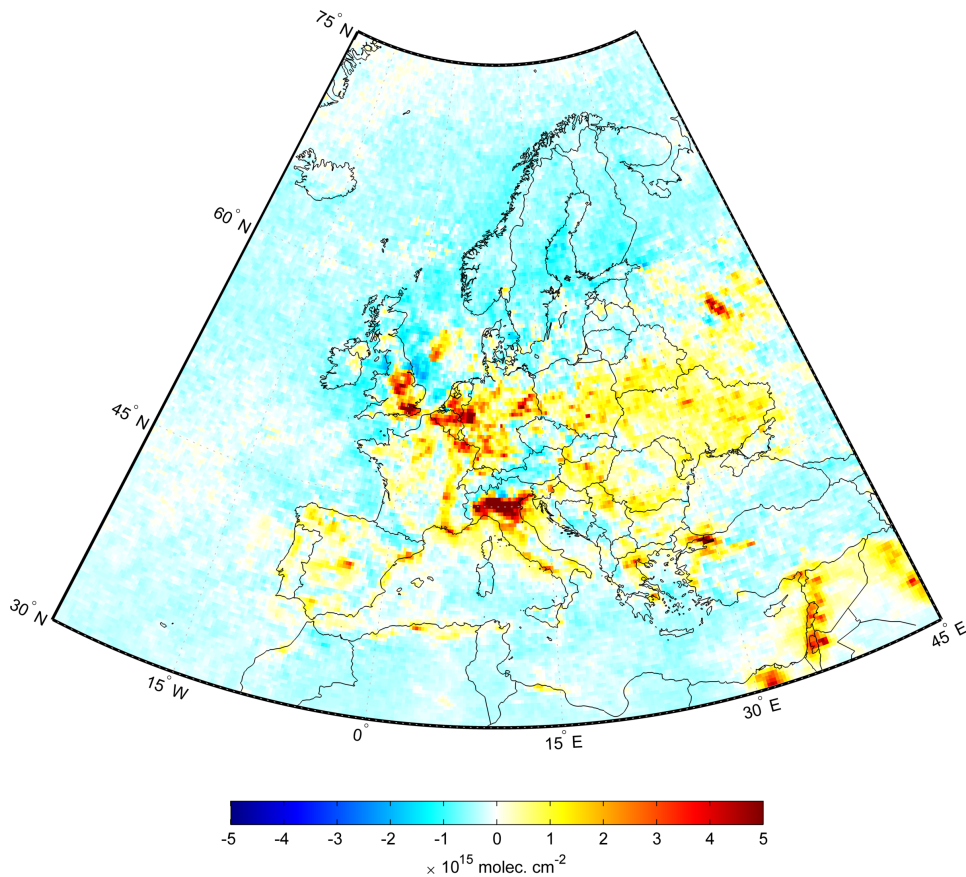


Figure 5 – Difference image of the mean annual NO_2 column retrieved from SCIAMACHY and OMI. The difference is calculated based on Equation 5. Note that both satellite instruments have significantly different overpass times (10:00 vs. 13:30 local time), which together with the diurnal cycle of NO_2 explain the majority of the inter-sensor biases.

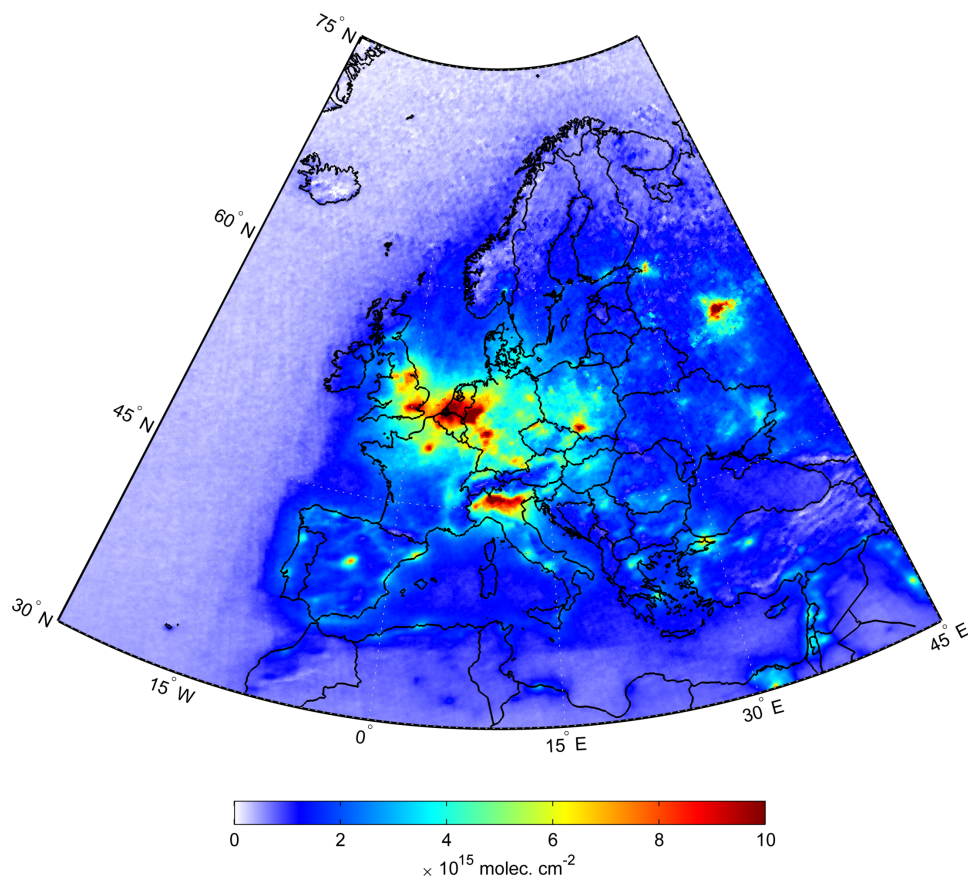


Figure 6 – The $0.1^\circ \times 0.1^\circ$ resolution OMINO2e product over Europe. Shown here is the 2009 annual mean tropospheric NO₂ concentration as computed from daily datasets.

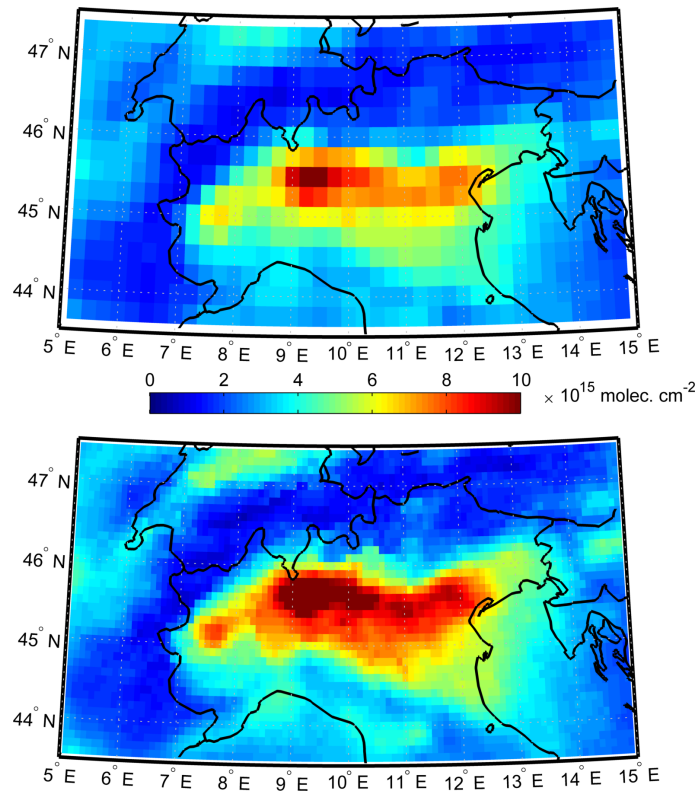


Figure 7 – Comparison of the 0.25 degree resolution OMNO2e product (top) with the 0.1 degree resolution OMNO2e product (bottom), shown for the Po valley region in Northern Italy. The higher resolution product clearly shows details not visible in the image of the 0.25 degree resolution product. The figures show the annual mean tropospheric NO₂ column in 2009.

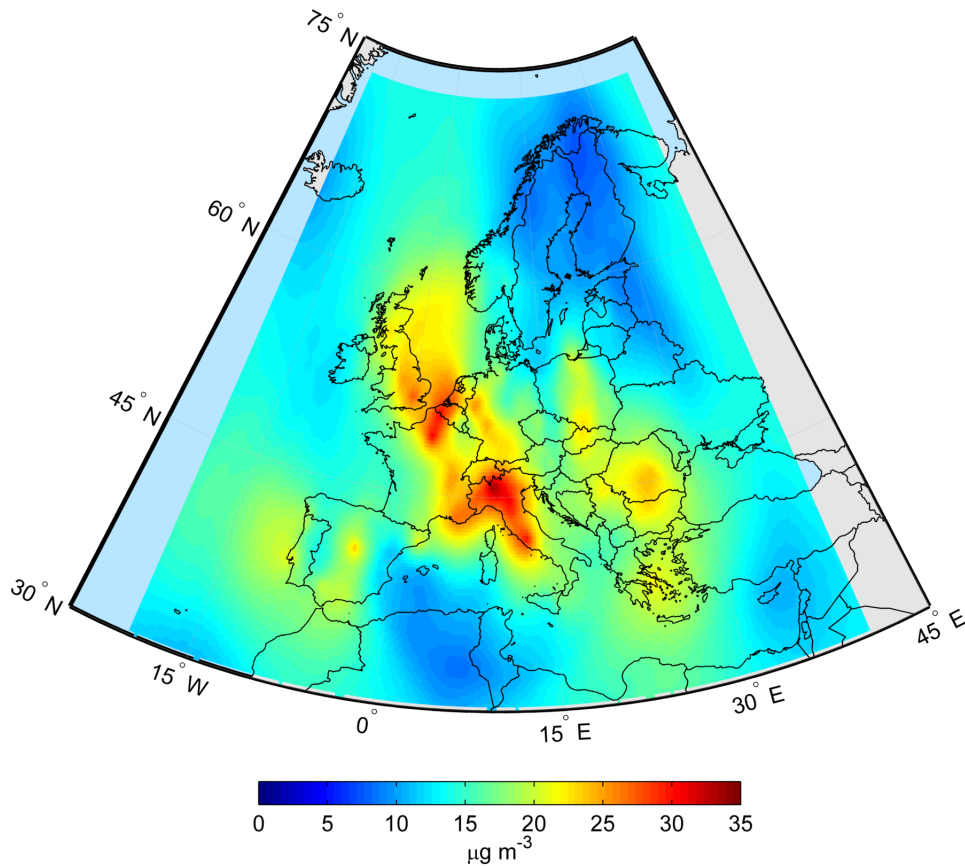


Figure 8 – Ordinary kriging of Airbase station data only. No auxiliary data was used in this approach.

4.2 Mapping using only station data

In order to establish a baseline indicating what type of map can be extracted from the Airbase station data alone and to thus be able to assess any additional potential of auxiliary datasets, ordinary kriging without any auxiliary data was carried out on the 2009 annual mean NO_2 concentrations observed at the stations. As mentioned before, only 90% of Airbase background stations selected for mapping were used for this purpose, while the remaining 10% of stations were considered exclusively for validation purposes. A combination of nugget effect and spherical semivariogram model was used to model the spatial autocorrelation of the data set.

Figure 8 shows the result. Due to not using a spatially distributed auxiliary dataset the spatial features displayed by the map are very smooth and lack detail. Significant hotspots in annual NO_2 concentration are visible of the Northern Italy area as well as Belgium and Northern France. However, the size

of the hotspots is significantly larger than would be expected and their shape is too smooth considering the generally rapid spatial gradients associated with NO₂ maps. The root mean squared error as calculated over the 10% of stations used for validation was found to be $RMSE = 9.1 \mu\text{g m}^{-3}$.

Obviously, this type of mapping without using any auxiliary data is not too helpful for mapping European-scale air quality as it can not deliver more detailed spatial patterns. However it can serve as a baseline against which to judge the mapping methods using additional auxiliary data, such as satellite observations or model output.

4.3 Mapping using station and satellite data

In order to provide an indication as to what extent satellite data of NO₂ can help improve European-scale mapping of air quality, OMI-based tropospheric column NO₂ data was subsequently used in the next step to complement the station measurements from Airbase as an auxiliary dataset. As described in detail in the methodology section, this was accomplished by establishing a correlation between the station-based NO₂ means and the mean satellite-based tropospheric columns as observed over each station.

Figure 9 shows a scatter plot indicating this correlation between the 2009 annual average NO₂ concentration at all background Airbase stations and the 2009 annual average tropospheric column extracted at each station location from the high-resolution annual average OMI dataset. A linear model was fitted to this dataset as $C_{OMI} = 1.89 + 0.12 \times C_{St}$, where C_{OMI} is the tropospheric column observed by the OMI instrument and C_{St} is the annual mean NO₂ concentration observed at each Airbase station. The R^2 value of the model was found to be close to 0.3.

At first glance this correlation might appear to be quite weak, however it needs to be considered that this analysis compares two parameters which have very different spatial and temporal scales. While the station observations provide an annual mean NO₂ value at the ground level and which is representative of only a very small area, the satellite provides the total number of NO₂ molecules at 14:00 local time, averaged not only over a 100 km² area but also integrated over the entire troposphere. Given these fundamental differences in spatial and temporal scales, the correlation seen in Figure 9 is quite remarkable.

The residuals resulting from the fitted linear regression were then subsequently plotted as an empirical semivariogram, which was then in turn modeled using a combined nugget effect of 64.3 and a Gaussian model with range 5.9 degrees and a sill of 18.9 (see Figure 10).

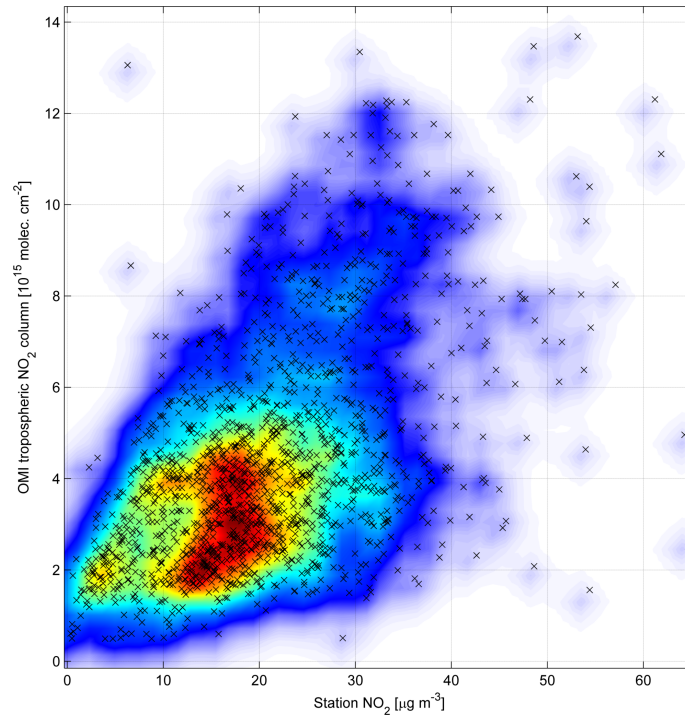


Figure 9 – Scatterplot of Airbase-derived annual mean 2009 station NO_2 concentration against the 2009 annual mean tropospheric NO_2 columns derived from the OMNO2e high-resolution product.

This semivariogram model was then used to kriging the residuals from the previously discussed linear regression over the entire study domain. This domain ranged from 20° N to 73° N and from 20° W to 40° E. A spatial resolution of 0.1° was used for the final grid.

Figure 11 shows the result of using station data together with OMI satellite data for mapping. The map indicates the annual mean NO_2 concentration in Europe with a spatial resolution of 0.1 degrees. In addition, regions of special interest in the map are highlighted in more detail in Figure 12.

Compared to Figure 8, Figure 11 shows significantly more detail. All major NO_2 hotspot over the Po valley in Northern Italy, the area of Belgium/Netherlands and western Germany, as well as the southern United Kingdom clearly show areas of high NO_2 concentration with the highest values found near the location of the major metropolitan areas. It should be noted that the areas over the oceans should be considered invalid in this map as they indicate low to moderate concentration when they should be close to zero. This erroneous behavior is due to the kriging approach used here which assigns a default variance (the nugget) to all areas without any station observations.

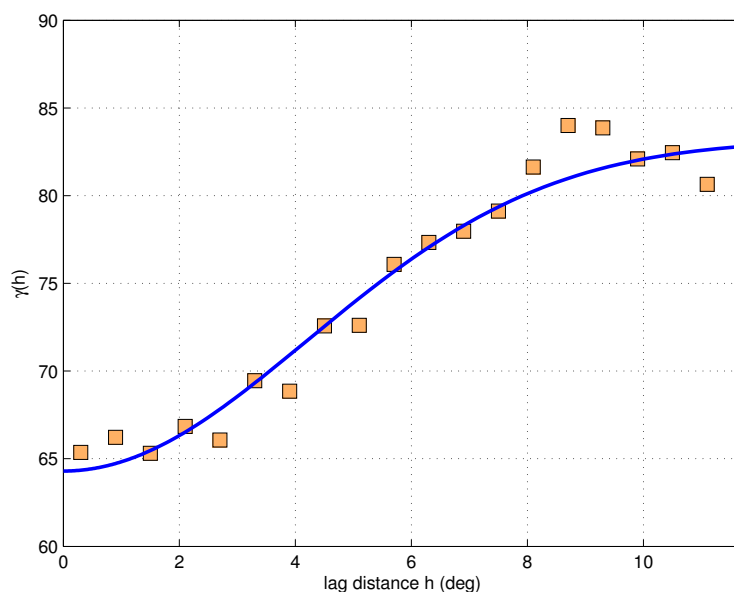


Figure 10 – Empirical and modeled semivariogram of the residuals. The model is a combination of a nugget effect of 64.3 and a gaussian model with range 5.9 and a sill of 18.9.

For this reason, only the land areas shown in this map should be considered as providing valid data.

Figure 12 shows the same map based on residual kriging of both station observations and OMI satellite data, however it provides more detail in several particular regions of interest. These regions are a) Belgium/Netherlands/Western Germany, b) the Po valley in Italy with the main hotspot north of Milan, c) the southeastern United Kingdom with the hotspot of London, and d) central Spain with the hotspot of Madrid.

The validation for this map resulted in an RMSE of $8.5 \mu\text{g m}^{-3}$, which is lower than the mapping carried out using solely station data. As expected, this indicates that the satellite dataset provides additional valuable information on spatial patterns.

4.4 Comparison of mapping techniques

The result of mapping NO_2 using station observations and satellite data as an auxiliary dataset was subsequently compared to the more traditional approach of using model output as an auxiliary variable, as it is currently applied for example by the operational ETC/ACM mapping routines described by Horálek et al. (2010). For this purpose, three more mapping approaches,

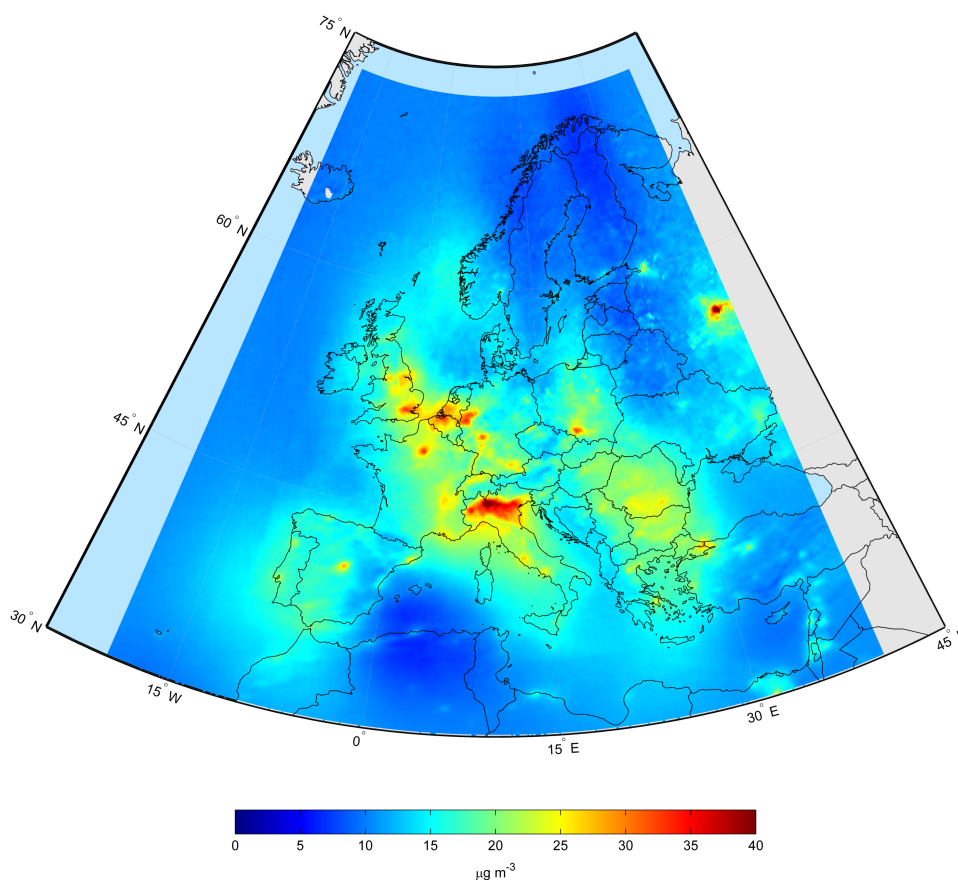


Figure 11 – Map of the 2009 annual average NO₂ concentration computed as the result from kriging station data from Airbase using the OMNO2e satellite product as an auxiliary dataset. The spatial resolution of the kriged product is 0.1 degrees or approximately 10 km.

all involving output from the CHIMERE chemical transport model as produced for the EC4MACS project, were tested. The first and simplest methodology consisted of using only the model output and to study how well the modeled concentrations were able to reproduce the concentrations observed at the set of validation stations. Secondly, the model output provided by EC4MACS was used as an auxiliary variable applying the same methodology as was described previously for using OMI satellite data. Thirdly, both model output and satellite data were used as two separate auxiliary datasets in a geostatistical framework involving residual kriging, thus testing if a combined use of these two auxiliary dataset can further improve the mapping accuracy.

Figure 13 shows the result of mapping European annual average NO₂ concentrations for 2009 using station data from Airbase and high-resolution model output from the CHIMERE model as an auxiliary variable. Overall, in terms of

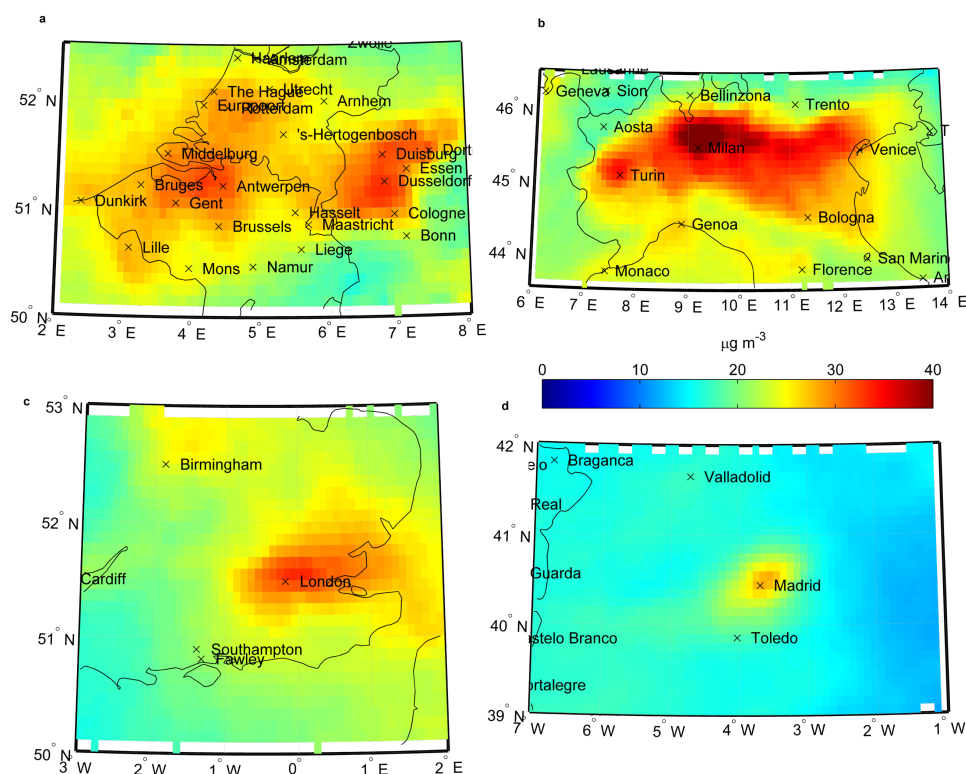


Figure 12 – As Figure 11 but showing more detail in the spatial patterns, for the regions of a) Belgium/Netherlands, b) Northern Italy, c) London, and d) Central Spain.

qualitative analysis of spatial patterns this approach produces a fairly similar map to the one obtained from using satellite data as an auxiliary variable (Figures 11 and 12). The very large NO₂ hotspots in the Po valley region of Northern Italy and in the region of the Netherlands are very well replicated by both approaches. A stark difference, however, is visible in terms of the number hotspots detected around smaller cities. While large metropolitan areas with very high NO_x emissions appear equally well in the maps derived from both approaches, only the map generated by the model-based approach also shows NO₂ hotspots for smaller cities.

This is for example visible in Germany, where the model-based map picks up several smaller cities which do not appear in the satellite-based map. This behavior is likely due to the still insufficient spatial resolution of the satellite instruments, which can not resolve small hotspots with a reasonable accuracy. In contrast, models can often make use of 1 km gridded emission inventories and information on point emissions sources and as such are able to more easily identify such small urban areas. Nonetheless, upcoming GMES satellite instruments will increase the available spatial resolution and are

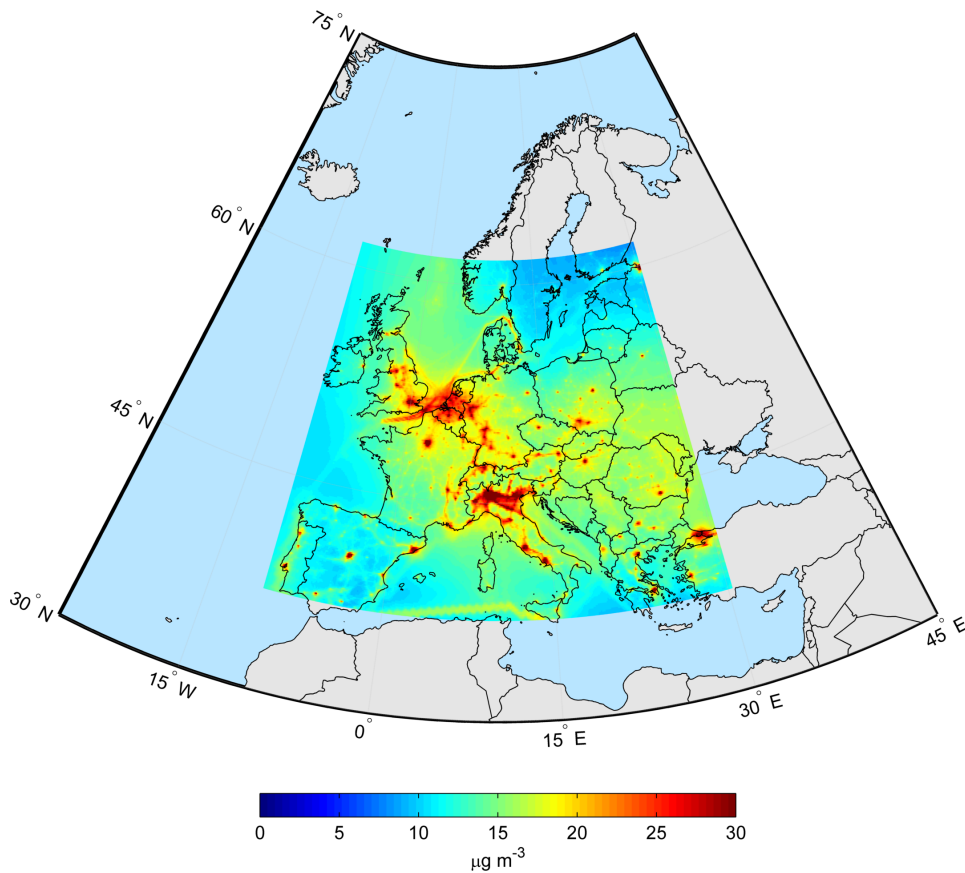


Figure 13 – Annual mean NO₂ concentration at ground level for the year 2009 as calculated from Airbase station data and EC4MACS project results using residual kriging.

thus bound to improve the capability of detecting smaller emission sources. One additional detail which is visible in the model-based map but not in the satellite-based map are shipping lanes. These appear very clearly in the model-based map in the Mediterranean, the North Sea, and, to some extent, in the Atlantic Ocean. Their existence is also based on the gridded emission inventory used for the model, whereas these features are not picked up by the satellite product. It should be noted, however, that the NO₂ signal of shipping lanes can be picked up by satellites as previous studies have shown (Richter, 2004; De Ruyter de Wildt et al., 2012), however this is mostly limited to extremely well defined lanes with extremely high traffic and thus emissions, such as in the Middle East and in Asia.

As a quantitative comparison, the root mean squared error (RMSE) statistics was used. It was calculated between the annual average NO₂ concentration at the entire set of validation stations and the NO₂ concentration indicated

Table 2 – Root mean squared error statistics for the different mapping approaches. The RMSE was computed over the randomly selected set of stations used only for validation, which were therefore not part of the kriging. This set of stations consisted of a total of 198 background stations throughout Europe.

Mapping method	RMSE [$\mu\text{g m}^{-3}$]
EC4MACS	10.9
AIRBASE only	9.1
AIRBASE and OMI	8.5
AIRBASE and EC4MACS	7.3
AIRBASE and OMI and EC4MACS	7.3

by the respective mapping approach, extracted from the grid exactly at the location of all stations. The set of randomly selected validation stations included approximately 10% of the original stations, which is equivalent to 198 stations in total.

Table 2 gives a quantitative comparison of the various mapping techniques and products tested here. Unsurprisingly, using only model output produces the highest error with a value of $10.9 \mu\text{g m}^{-3}$. This is due to the fact that no actual observations from stations are incorporated in the modelling. When a geostatistical approach (ordinary kriging) is applied to only Airbase station observations without using any auxiliary dataset, the RMSE of the predictions is reduced to $9.1 \mu\text{g m}^{-3}$.

When satellite data from the OMI-based high-resolution OMNO2e product is used as an auxiliary dataset in the kriging process, the RMSE between the annual NO_2 means at the set of validation stations and the corresponding prediction, decreases even further to a value of $8.5 \mu\text{g m}^{-3}$. This clearly demonstrates that, despite fundamentally different spatial and temporal measurement scales, satellite data on tropospheric column can improve the prediction accuracy of a geostatistical mapping process.

Finally, when high-resolution model output from a chemical transport model such as CHIMERE was used as an auxiliary dataset, the RMSE decreased even further to a value of $7.3 \mu\text{g m}^{-3}$, indicating that the high-resolution model output is best suited to provide information about the spatial patterns of NO_2 distribution in Europe. When both satellite data and model output are used at the same time as auxiliary variables, the RMSE does not improve any further, indicating that the satellite can not provide additional spatial information on NO_2 distributions beyond that which the model output can offer.

5 Conclusions

5.1 Summary

A multitude of data products on air quality are currently available from various satellite instruments. Both the amount of data and its quality is even bound to increase in future with the launch of the series of Sentinel satellite within the framework of the Global Monitoring of Environment and Security (GMES) initiative.

Based on this growing importance of spaceborne data for air quality related applications it is highly desirable to study the impact of satellite data on currently existing air quality mapping techniques. In this report, the potential of using satellite-based NO₂ data as an auxiliary variable for mapping air quality at the European scale using geostatistical techniques was investigated. In a first step, an inter-comparison between tropospheric NO₂ column products from two different satellite instruments was carried out and the characteristics of the different data products were evaluated in order to select the most suitable candidate. Based on various criteria a 0.1 degree spatial resolution NO₂ product based on the Ozone Mapping Instrument (OMI) was selected here for further analysis.

In order to establish a baseline, ordinary kriging using only station data was carried out at the European scale. This allowed for an estimate of what type of mapping accuracy can be achieved using solely station data. Subsequently, a linear regression model was established between the annual average NO₂ station observations and the satellite-based tropospheric columns extracted over the located of all stations. The residuals found in this model were then kriged using the OMI satellite product as an auxiliary variable. This mapping technique was then subsequently compared to a similar mapping approach using the output of a high-resolution chemical transport model as an auxiliary variable.

The results of the study indicate that satellite data can be very useful as an auxiliary variable in mapping European air quality. Using tropospheric column NO₂ data acquired by the OMI instrument provided significantly better mapping results (both qualitatively as well as quantitatively) than geostatistical interpolation of station data alone.

However, while the satellite data investigated here had a positive impact on the mapping procedure, it was not able to achieve the same level of impact as using the output of a high-resolution chemical transport model as an auxiliary variable. The latter was able to produce lower root mean squared errors when validated against a subset of the stations. To some extent this behavior is to be expected. The model provides ground-level concentrations and is based

on highly detailed emission inventories, thus capturing the spatial detail and sharp gradients in NO_x emissions. In contrast, the satellite dataset provides the annual average total number of molecules in the entire tropospheric column at about 14:00 in the afternoon over an area of approximately 100 km^2 . As such, the satellite dataset is obviously not expected to completely replicate the spatial detail that can be provided by the model.

Nonetheless, the satellite data provides very useful information. The model data used here represents a best case scenario, as it was available at a comparatively high spatial resolution. Due to the extremely high demands on computational resources, such high resolution model data is at the present time not produced operationally and is therefore only available for individual years or certain periods. Satellites on the other hand provide an operational system for monitoring the Earth's atmosphere and have now been providing continuous air quality information since the mid 1990s and are expected to provide even further improved, operational products over the next several decades.

In such cases, when high-resolution model output is not available or can not feasibly be used for air quality mapping purposes, satellite data of the NO_2 tropospheric column can provide a readily available proxy for spatially distributed auxiliary data, thus supporting the mapping process and decreasing the mapping uncertainty compared to geostatistically interpolating station data alone.

While running atmospheric chemistry models at high spatial and temporal resolutions is currently challenging due to the computational cost associated with such activities, this situation is likely to improve in the future as computing power increases and high-performance computing becomes ubiquitous. With this situation in mind it will become critical to further investigate the potential of assimilating satellite data in models.

5.2 Recommendations

The 0.1 degree resolution OMNO2e product acquired by the OMI instrument and produced by NASA is recommended as the currently most suitable NO_2 satellite product for European-scale air quality mapping. The spatial resolution of the product is very similar to the 10 km spatial resolution currently applied in the ETC/ACM operational mapping procedure. Furthermore, in contrast to for example SCIAMACHY, the OMI sensor is still operational and delivers a continuous data stream.

While it was shown that satellite estimates of NO_2 can be helpful for mapping European-scale air quality, the methodology used for this study was quite simplified compared to the operational mapping system being used by the

ETC/ACM (Horálek et al., 2007, 2008, 2010; De Smet et al., 2009, 2010; Denby et al., 2010, 2011a,b). Future work could investigate the use of the 0.1 degree resolution OMNO2e dataset within the operational ETC/ACM air quality mapping methodology. This could allow for rigorous testing of the satellite dataset within the existing comprehensive approach which has been refined over many years.

Future satellite instruments designed for providing information on atmospheric composition will allow for the acquisition of data at significantly improved spatial and temporal resolution. Within the framework of the GMES initiative, this includes primarily the Sentinel-5 precursor (TROPOMI) (van Weele et al., 2008; Veefkind et al., 2012) which will be launched in March 2015, the geostationary Sentinel-4 mission to be launched in 2019 and the Sentinel-5 mission to be launched in the 2020 time frame (Ingmann et al., 2012; Berger et al., 2012). It is recommended to study the potential of these new missions with respect to further improving air quality mapping and potentially even their use for more urban-scale mapping than can be achieved at present.

Acknowledgements

We are very grateful to Lok Lamsal at NASA Goddard for providing the version 3.0 OMI NO₂ product, and in particular the experimental 0.1 degree NO₂ product. We would further like to thank Laure Malherbe, Laurence Rouil, Bertrand Bessagnet and Etienne Terrenoire from INERIS for providing access to the high resolution model data.

References

- Aschbacher, J. and Milagro-Pérez, M. P. (2012). The European Earth monitoring (GMES) programme: Status and perspectives. *Remote Sensing of Environment*, 120(2012):3–8.
- Berger, M., Moreno, J., Johannessen, J. A., Levelt, P. F., and Hanssen, R. F. (2012). ESA's sentinel missions in support of Earth system science. *Remote Sensing of Environment*, 120:84–90.
- Bessagnet, B., Hodzic, A., Vautard, R., Beekmann, M., Cheinet, S., Honoré, C., Liousse, C., and Rouil, L. (2004). Aerosol modeling with CHIMERE - preliminary evaluation at the continental scale. *Atmospheric Environment*, 38(18):2803–2817.
- Boersma, K. F., Eskes, H. F., and Brinksma, E. J. (2004). Error analysis for tropospheric NO₂ retrieval from space. *Journal of Geophysical Research*, 109(D4).
- Boersma, K. F., Eskes, H. J., Dirksen, R. J., van der A, R. J., Veefkind, J. P., Stammes, P., Huijnen, V., Kleipool, Q. L., Sneep, M., Claas, J., Leitão, J., Richter, A., Zhou, Y., and Brunner, D. (2011). An improved tropospheric NO₂ column retrieval algorithm for the Ozone Monitoring Instrument. *Atmospheric Measurement Techniques*, 4:1905–1928.
- Boersma, K. F., Eskes, H. J., Veefkind, J. P., Brinksma, E. J., van der A, R. J., Sneep, M., van den Oord, G. H. J., Levelt, P. F., Stammes, P., Gleason, J. F., and Bucsela, E. J. (2007). Near-real time retrieval of tropospheric NO₂ from OMI. *Atmospheric Chemistry and Physics*, 7:2103–2118.
- Bovensmann, H., Burrows, J. P., Buchwitz, M., Frerick, J., Noël, S., Rozanov, V. V., Chance, K. V., and Goede, a. P. H. (1999). SCIAMACHY: Mission Objectives and Measurement Modes. *Journal of the Atmospheric Sciences*, 56(2):127–150.
- Bucsela, E., Celarier, E., Wenig, M., Gleason, J., Veefkind, J., Boersma, K., and Brinksma, E. (2006). Algorithm for NO₂ vertical column retrieval from the ozone monitoring instrument. *IEEE Transactions on Geoscience and Remote Sensing*, 44(5):1245–1258.
- Bucsela, E. J. (2012). A new algorithm for retrieval of stratospheric and tropospheric NO₂ from nadir satellite instruments. *in preparation*.
- Burrows, J. P., Weber, M., Buchwitz, M., Rozanov, V., Ladstätter-Weiß enmayer, A., Richter, A., DeBeek, R., Hoogen, R., Bramstedt, K., Eichmann, K.-U., Eisinger, M., and Perner, D. (1999). The Global Ozone Monitoring Experiment (GOME): Mission Concept and First Scientific Results. *Journal of the Atmospheric Sciences*, 56(2):151–175.

- Chance, K. (2002). OMI Algorithm Theoretical Basis Document - Volume IV: OMI Trace Gas Algorithms. Technical Report ATBD-OMI-04, Smithsonian Astrophysical Observatory, Cambridge, MA, United States.
- Cressie, N. A. C. (1993). *Statistics for spatial data*. Wiley-Interscience, New York.
- De Ruyter de Wildt, M., Eskes, H., and Boersma, K. F. (2012). The global economic cycle and satellite-derived NO₂ trends over shipping lanes. *Geophysical Research Letters*, 39(1):2–7.
- De Smet, P., Horálek, J., Conková, M., Kurfürst, P., De Leeuw, F., and Denby, B. (2010). European air quality maps of ozone and PM₁₀ for 2008 and their uncertainty analysis. Technical Report ETC/ACC Technical Paper 2010/10, European Topic Centre on Air and Climate Change, Bilthoven, Netherlands.
- De Smet, P., Horálek, J., Conková, M., Kurfürst, P., Leeuw, F. D., and Denby, B. (2009). European air quality maps of ozone and PM 10 for 2006 and their uncertainty analysis. Technical Report ETC/ACC Technical Paper 2008/8.
- Denby, B., Gola, G., de Leeuw, F., de Smet, P., and Horálek, J. (2011a). Calculation of pseudo PM_{2.5} annual mean concentrations in Europe based on annual mean PM₁₀ concentrations and other supplementary data. Technical Report ETC/ACC 2010/9, European Topic Centre on Air and Climate Change, Bilthoven, Netherlands.
- Denby, B., Sundvor, I., Cassiani, M., de Smet, P., de Leeuw, F., and Horálek, J. (2010). Spatial mapping of ozone and SO₂ trends in Europe. *The Science of the total environment*, 408(20):4795–806.
- Denby, B. R., Horálek, J., Smet, P. D., and Leeuw, F. D. (2011b). Mapping annual mean PM_{2.5} concentrations in Europe: application of pseudo PM_{2.5} station data. Technical Report ETC/ACM Technical Paper 2011/5.
- Dentener, F., van Weele, M., Krol, M., Houweling, S., and van Velthoven, P. (2003). Trends and inter-annual variability of methane emissions derived from 1979-1993 global CTM simulations. *Atmospheric Chemistry and Physics*, 3:73–88.
- Fagerli, H., Simpson, D., and Tsyro, S. (2004). Unified EMEP model: Updates. In Tarrasón, L., Fagerli, H., Jonson, J. E. J., Klein, H., van Loon, M., Simpson, D., Tsyro, S., Vestreng, V., Wind, P., Posch, M., Solberg, S., Spranger, T., Cuvelier, K., Thunis, P., and White, L., editors, *Transboundary Acidification, Eutrophication and Ground Level Ozone in Europe: EMEP Status Report 2004*, pages 11–18.

- Glantz, P., Kokhanovsky, A., von Hoyningen-Huene, W., and Johansson, C. (2009). Estimating PM_{2.5} over southern Sweden using space-borne optical measurements. *Atmospheric Environment*, 43(36):5838–5846.
- Goovaerts, P. (1997). *Geostatistics for natural resources evaluation*. Oxford University Press, New York.
- Gottwald, M., Bovensmann, H., Lichtenberg, G., Noel, S., von Bargen, A., Slijkhuis, S., Piters, A., Hoogeveen, R., von Savigny, C., Buchwitz, M., Kokhanovsky, A., Richter, A., Rozanov, A., Holzer-Popp, T., Bramstedt, K., Lambert, J.-C., Skupin, J., Wittrock, F., Schrijver, H., and Burrows, J. (2006). *SCIAMACHY - Monitoring the Changing Earth's Atmosphere*. DLR, Institute fuer Methodik der Fernerkundung (IMF).
- Horálek, J., Denby, B., Smet, P. D., Leeuw, F. D., Kurfürst, P., Swart, R., and van Noije, T. (2007). Spatial mapping of air quality for European scale assessment. Technical Report ETC/ACC 2006/6, European Topic Centre on Air and Climate Change, Bilthoven, Netherlands.
- Horálek, J., Smet, P. D., Leeuw, F. D., Conková, M., Denby, B., and Kurfürst, P. (2010). Methodological improvements on interpolating European air quality maps. Technical Report ETC/ACC 2009/16, European Topic Centre on Air and Climate Change, Bilthoven, Netherlands.
- Horálek, J., Smet, P. D., Leeuw, F. D., Denby, B., Kurfürst, P., and Swart, R. (2008). European air quality maps for 2005 including uncertainty analysis. Technical Report ETC/ACC Technical Paper 2007/7.
- Ingmann, P., Veiðelmann, B., Langen, J., Lamarre, D., Stark, H., and Courrèges-Lacoste, G. B. (2012). Requirements for the GMES Atmosphere Service and ESA's implementation concept: Sentinels-4/-5 and -5p. *Remote Sensing of Environment*, 120:58–69.
- Isaaks, E. H. and Srivastava, R. M. (1989). *Applied geostatistics*. Oxford University Press, New York.
- Levelt, P., van den Oord, G., Dobber, M., Malkki, A., Stammes, P., Lundell, J., and Saari, H. (2006). The Ozone Monitoring Instrument. *IEEE Transactions on Geoscience and Remote Sensing*, 44(5):1093–1101.
- Munro, R., Eisinger, M., Anderson, C., Callies, J., Corpaccioli, E., Lang, R., Lefebvre, A., Livschitz, Y., and Albiñana Perez, A. (2006). GOME-2 on MetOp. In *Proceedings of the 2006 EUMETSAT Meteorological Satellite Conference*, Helsinki, Finland.
- OMI Team (2012). Ozone Monitoring Instrument (OMI) Data User's Guide. Technical Report OMI-DUG-5.0.

- Popp, C., Brunner, D., Damm, A., Van Roozendaal, M., Fayt, C., and Buchmann, B. (2012). High resolution NO₂ remote sensing from the Airborne Prism EXperiment (APEX) imaging spectrometer. *Atmospheric Measurement Techniques Discussions*, 5(2):2449–2486.
- Richter, A. (2004). Satellite measurements of NO₂ from international shipping emissions. *Geophysical Research Letters*, 31(23):4–7.
- Richter, A. and Burrows, J. P. (2002). Tropospheric NO₂ from GOME measurements. *Advances in Space Research*, 29(11):1673–1683.
- Simpson, D., Fagerli, H., Jonson, J., Tsyro, S., and Wind, P. (2003). Transboundary Acidification, Eutrophication and Ground Level Ozone in Europe - Part I - Unified EMEP Model Description. Technical Report 1/2003, Norwegian Meteorological Institute, Oslo, Norway.
- van Weele, M., Levelt, P., Aben, I., Veefkind, P., Dobber, M., Eskes, H., Houweling, S., Landgraf, J., and Noordhoek, R. (2008). Science Requirements Document for TROPOMI. Technical report, KNMI, De Bilt, Netherlands.
- Vautard, R., Beekmann, M., Roux, J., and Gombert, D. (2001). Validation of a hybrid forecasting system for the ozone concentrations over the Paris area. *Atmospheric Environment*, 35(14):2449–2461.
- Veefkind, J., Aben, I., McMullan, K., Förster, H., de Vries, J., Otter, G., Claas, J., Eskes, H., de Haan, J., Kleipool, Q., van Weele, M., Hasekamp, O., Hoogeveen, R., Landgraf, J., Snel, R., Tol, P., Ingmann, P., Voors, R., Kruizinga, B., Vink, R., Visser, H., and Levelt, P. (2012). TROPOMI on the ESA Sentinel-5 Precursor: A GMES mission for global observations of the atmospheric composition for climate, air quality and ozone layer applications. *Remote Sensing of Environment*, 120:70–83.
- Wackernagel, H. (2003). *Multivariate geostatistics: an introduction with applications*. Springer, Berlin, Heidelberg, New York.